

# Retrieving a disrupted gene encoding phospholipase A for fibre enhancement in allotetraploid cultivated cotton

Lei Fang<sup>1,2,\*</sup>, Zhiyuan Zhang<sup>2,3,†</sup>, Ting Zhao<sup>1,2,†</sup>, Na Zhou<sup>3</sup>, Huan Mei<sup>1</sup>, Xingqi Huang<sup>4</sup>, Fang Wang<sup>3</sup>, Zhanfeng Si<sup>1</sup>, Zegang Han<sup>1</sup>, Shan Lu<sup>4</sup>, Yan Hu<sup>1,2</sup>, Xueying Guan<sup>1,2</sup> and Tianzhen Zhang<sup>1,2,\*</sup>

<sup>1</sup>Zhejiang Provincial Key Laboratory of Crop Genetic Resources, Institute of Crop Science, Plant Precision Breeding Academy, College of Agriculture and Biotechnology, Zhejiang University, Hangzhou, China

<sup>2</sup>Hainan Institute of Zhejiang University, Sanya, China

<sup>3</sup>National Key Laboratory of Crop Genetics & Germplasm Enhancement, Cotton Research Institute, Nanjing Agricultural University, Nanjing, China

<sup>4</sup>State Key Laboratory of Pharmaceutical Biotechnology, School of Life Sciences, Nanjing University, Nanjing, China

Received 9 March 2022;

revised 18 May 2022;

accepted 23 May 2022.

\*Correspondence Lei Fang (Tel +0571 88982315; fax +0571 88982315; email fangl@zju.edu.cn); Tianzhen Zhang (Tel +0571 88982870; fax +0571 88982870; email cotton@zju.edu.cn)

†These authors contributed equally to this work.

## Summary

After polyploidization originated from one interspecific hybridization event in *Gossypium*, *Gossypium barbadense* evolved to produce extra-long staple fibres than *Gossypium hirsutum* (Upland cotton), which produces a higher fibre yield. The genomic diversity between *G. barbadense* and *G. hirsutum* thus provides a genetic basis for fibre trait variation. Recently, rapid accumulation of gene disruption or deleterious mutation was reported in allotetraploid cotton genomes, with unknown impacts on fibre traits. Here, we identified gene disruptions in allotetraploid *G. hirsutum* (18.14%) and *G. barbadense* (17.38%) through comparison with their presumed diploid progenitors. Relative to conserved genes, these disrupted genes exhibited faster evolution rate, lower expression level and altered gene co-expression networks. Within a module regulating fibre elongation, a hub gene experienced gene disruption in *G. hirsutum* after polyploidization, with a 2-bp deletion in the coding region of *GhNPLA1D* introducing early termination of translation. This deletion was observed in all of the 34 *G. hirsutum* landraces and 36 *G. hirsutum* cultivars, but not in 96% of 57 *G. barbadense* accessions. Retrieving the disrupted gene *GhNPLA1D* using its homoeolog *GhNPLA1A* achieved longer fibre length in *G. hirsutum*. Further enzyme activity and lipids analysis confirmed that *GhNPLA1A* encodes a typical phospholipase A and promotes cotton fibre elongation via elevating intracellular levels of linolenic acid and 34:3 phosphatidylinositol. Our work opens a strategy for identifying disrupted genes and retrieving their functions in ways that can provide valuable resources for accelerating fibre trait enhancement in cotton breeding.

**Keywords:** *Gossypium*, Disrupted gene, Phospholipase A, Fibre elongation, Linolenic acid.

## Introduction

Two allotetraploid cotton species were domesticated independently, each offering superior traits relative to their diploid ancestors. More specifically, *Gossypium hirsutum* ( $2n = 4x = 52$ , AD<sub>1</sub>) is characterized by high-yield properties and its cultivars dominate more than 90% of worldwide cotton production, while *G. barbadense* ( $2n = 4x = 52$ , AD<sub>2</sub>) is characterized by strong and fine fibres with extra-long staples, which accounts for less than 10% of cotton global production (Wendel *et al.*, 2010). The polyploid vigour and hybrid vigour of fibre traits in allotetraploid cotton cultivars result from the orchestrated effects of genome structural variations after polyploidization, in addition to natural and human selection (Adams and Wendel, 2005). However, the genetic and molecular basis for the interspecies divergence in fibre traits remains largely unknown, which presents a barrier in breeding cotton with superior fibre traits.

Previously, we characterized interspecies introgression events between *G. hirsutum* and *G. barbadense*, which had significant impacts on fibre yield and quality traits in *G. barbadense* populations (Fang *et al.*, 2021). Notably, after polyploidization/

whole-genome duplication (WGD), some of the redundant genes were lost over the course of a few million years (Lynch and Conery, 2000). The most recent evolutionary analysis on the *Gossypium* genus reported that disrupted genes, also termed genes with deleterious mutations, have accumulated faster in allotetraploid cotton than in diploid species (Conover and Wendel, 2022). However, the precise effects of these disrupted genes on fibre traits have yet to be elucidated.

Cotton fibre comprises single-celled trichomes derived from the ovule epidermis, and its development consists of four overlapping stages: initiation, rapid elongation, secondary wall thickening and maturation (Chen and Guan, 2011; Graves and Stewart, 1988; Kim and Triplett, 2001). Both transcriptome and metabolism analyses have indicated that lipid transportation and metabolic processing occur proactively during the initiation and elongation stages (Gou *et al.*, 2007; Guan *et al.*, 2011; Hu *et al.*, 2019). During rapid elongation, the primary cell wall of the fibre is extended through rapid assembly of plasma membranes and vacuole development, which imposes a huge demand for phospholipids (Wanjie *et al.*, 2005). Phospholipids and their derivatives such as linolenic acid, 34:3 phosphatidylinositol (PI)

and PI-4 monophosphate also promote cotton fibre elongation in their roles as signal molecules (Liu *et al.*, 2015). Therefore, the network regulating phospholipid metabolism also plays a critical role in cotton fibre development, though it yet remains understudied.

Here, we characterized the disrupted genes in allotetraploid cotton species *G. hirsutum* and *G. barbadense* by comparing the coding sequences and protein structures of orthologs with their respective progenitor diploids. Disrupted genes showed significantly lower expression levels than conserved genes, and variation in their alternative expression was associated with fibre development stages in co-expression networks, with enrichment of genes pertaining to fatty acid metabolic regulation. We further investigated the gene identified as a hub gene of fibre development, *GhNPLA1* (novel cotton phospholipase A in *G. hirsutum*), which encodes a phospholipase A. In *G. hirsutum* populations, *GhNPLA1D* (*GhNPLA1* from D subgenome) is disrupted by a 2-bp deletion and exhibits low transcription level. We found that ectopic expression of *GhNPLA1A* (*GhNPLA1* from A subgenome) can promote fibre elongation in transgenic lines of upland cotton. Enzyme activity and cotton fibre culture assays further demonstrated that the substrate of *GhNPLA1A* regulates fibre elongation directly. Thus, our study provides a strategy for trait enhancement of allopolyploid crops through the retrieval of disrupted genes.

## Results

### Identification and evolutionary trajectory of disrupted genes in the *Gossypium* lineage

To estimate the number of genes disrupted during cotton polyploidization and speciation, we utilized pairwise whole-genome alignments of each allotetraploid and its presumed progenitor diploid genomes (Figure 1a). Using ANNOVAR (Wang *et al.*, 2010) to annotate the genomic variation, a total of 17 925 variations in *G. hirsutum* and 17 886 in *G. barbadense* resulted in gene disruption through frameshift insertion (FI), frameshift deletion (FD), stop codon gain (SG) or stop codon loss (SL) (Table S1). Most genomic variations (97.62% in *G. hirsutum* and 96.63% *G. barbadense*) were confirmed by another software SnpEff (Cingolani *et al.*, 2012), indicating high accuracy of genomic variation annotations. Disruption most frequently occurred through a SG event, followed by FD, FI and SL (Figure S1). We further constructed gene disruption maps of the allotetraploids, which contained 13 200 disrupted genes in *G. hirsutum* and 13 049 disrupted genes in *G. barbadense* (Figure S2).

The disrupted genes constituted 16%–17% of the genome, based on a set of 20 096 orthologous gene pairs (Table S2). A total of 2921 disrupted genes shared between *G. hirsutum* and *G. barbadense* (*Gh-Gb*) (1289 from the A subgenome [At] and 1632 from the D subgenome [Dt]) were identified as related to *Gossypium* polyploidization (Figure 1b). Additionally, 1318 *Gh*-specific disrupted genes and 1172 *Gb*-specific disrupted genes were identified as related to allotetraploid speciation (Figure 1b, c and Table S2).

Disrupted genes related to polyploidization were found to have significantly higher average non-synonymous (Ka)/synonymous (Ks), Ka, and Ks values than those related to *Gb-Gh* speciation (Figure 1d and Figure S3). Synonymous substitution seems to be mainly neutral, and the disrupted genes related to polyploidization harboured more synonymous substitutions; this is consistent

with previous studies of bacteria, in which gene loss occurs in a clocklike, time-dependent manner (Snel *et al.*, 2002).

### Alternative expression of disrupted genes is associated with lipid metabolic progress during fibre development

We further evaluated the effect of gene disruption events on expression levels in different tissues (Table S3). In all 11 tissues examined, the average expression level of disrupted genes was significantly lower regardless of whether genes related to polyploidization or to *Gb-Gh* speciation than the average expression of conserved genes ( $P < 2.2 \times 10^{-16}$ , Wilcoxon test) (Figure 2a, b). This trend is similar to the expression patterns of pseudogenes in *Arabidopsis*, which are on average shorter and less expressed than conserved genes (Yang *et al.*, 2011).

Most disrupted genes (96.39% in *G. hirsutum* and 96.87% in *G. barbadense*) were found to be transcribed in the examined tissues. This raises a question as to whether a disrupted gene affects the functional networks of transcripts. To examine this possibility, we selected the homoeologous gene pairs with a disrupted gene and constructed their interaction networks using weighted gene co-expression network analysis (WGCNA) using 20 tissues from *G. hirsutum* and *G. barbadense*, respectively (Table S3). In quantifying the alterations in regulatory networks, we proposed three possible shared network patterns to exist between the A and D subgenomes: whole-share (index = 100%), part-share (0% < index < 100%) and zero-share (index = 0%) (method adapted from Arsovski *et al.*, 2015; Figure 2c). The homoeologous gene pairs were classified as either single-disrupted or double-disrupted depending on whether disruption occurred in only one subgenome or in both subgenomes when considering one-to-one homoeolog genes. The comparisons included 304 and 289 double-disrupted genes and 3631 and 3515 single-disrupted genes in *G. hirsutum* and *G. barbadense*, respectively (Table S4). The double-disrupted genes showed significantly lower correlation coefficients (*G. hirsutum* = 0.57, *G. barbadense* = 0.58) than either single-disrupted genes (*G. hirsutum* = 0.64; *G. barbadense* = 0.65,  $P < 2.2 \times 10^{-16}$ ) or conserved genes (*G. hirsutum* = 0.71; *G. barbadense* = 0.71,  $P < 2.2 \times 10^{-16}$ ) (Figure S4).

Through the WGCNA, 7,801,385 connections were identified among the 20 096 one-to-one homoeologous genes. In *G. hirsutum*, the shared network index was significantly decreased by 15% in single-disrupted genes (mean *G. hirsutum* = 0.34,  $P < 2.2 \times 10^{-16}$ , Wilcoxon test) and by 30% in double-disrupted genes (mean *G. hirsutum* = 0.28,  $P < 2.2 \times 10^{-16}$ , Wilcoxon test) when compared to conserved genes (mean *G. hirsutum* = 0.40). Similar result was observed in *G. barbadense* (Figure 2c). Interestingly, 450 single-disrupted genes were involved in extremely asymmetrical or altered networks (zero-share index = 0%). In *G. hirsutum*, the 20 096 homoeologous genes were grouped into 17 modules, of which six were related to ovule and fibre development (red, yellow green, dark turquoise, green, blue2, and lightpink4;  $p < 0.05$ ) (Figure 2d; Figure S5). In *G. barbadense*, these homoeologous genes were grouped into 12 modules; 6 of 12 were related to ovule and fibre development (pink, darkorange2, mediumpurple3, black, orangered3, and palevioletred2;  $p < 0.05$ ) (Figure S6). For Gene Ontology terms, the 1819 genes in module blue2 were enriched in the fatty acid metabolic process (GO:0006631) and regulation of cell growth (GO:0001558) in *G. hirsutum* (Figure 2e, Tables S5 and S6). Interestingly, 55 fibre-related genes were identified as single-disrupted and involved in an extremely alternated co-expression network with a share index

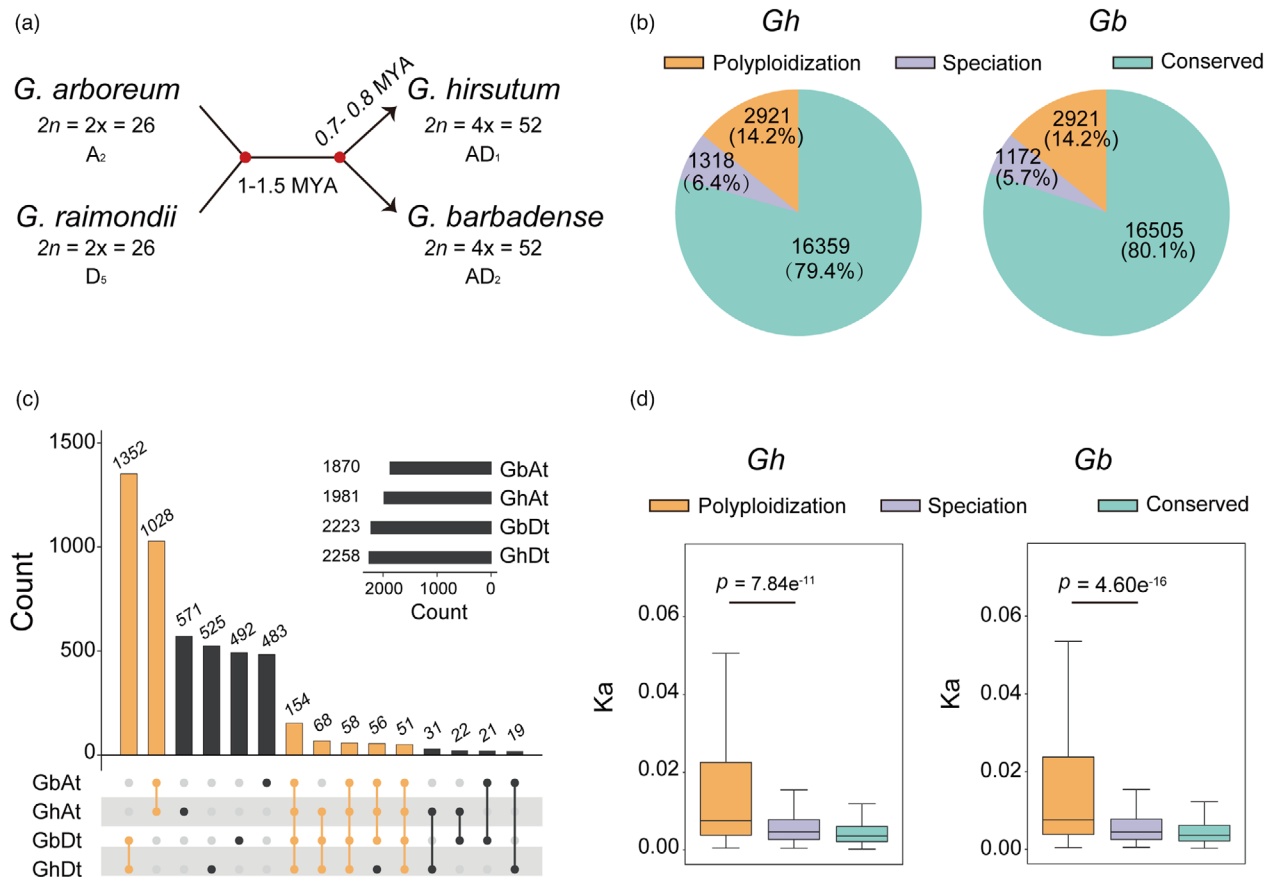


**Figure 1** Identification of disrupted genes in *Gossypium*. (a) Schematic chart describing the materials of the diploids *Gossypium arboreum* ( $A_2$  genome,  $Ga$ ) and *Gossypium raimondii* ( $D_5$  genome,  $Gr$ ) and the tetraploids *Gossypium hirsutum* ( $AD_1$  genome,  $Gh$ ) and *Gossypium barbadense* ( $AD_2$  genome,  $Gb$ ). Numbers indicate genome divergence times. (b) Pie chart showing the proportion and number of disrupted genes associated with polyploidization and speciation. (c) Numbers indicate the genes disrupted in polyploidization and speciation. Bottom, numbers of disrupted genes with one-to-one relationships. Dots indicate disrupted genes. Lines indicate disrupted genes common in given species. (d) Box plot comparing the evolution of disrupted genes in polyploidization and speciation as indicated by synonymous substitution rate ( $K_s$ ). Centre line, median; box limits, upper and lower quartiles; whiskers, 1.5 $\times$  the interquartile range (\*\*\* $p < 0.001$ , \*\* $p < 0.01$  and \* $p < 0.05$ , two-tailed Wilcoxon's test).

of 0% (Table S7). Taken together, our results indicate that the destruction of gene structure also affects the related co-expression or regulatory networks.

### The hub gene with disrupted homologous pair encoding a novel phospholipase A is associated with cell elongation

Among 55 fibre-related genes in the module blue 2, the gene *GH\_A05G4329* (*GhNPLA1A*) was ranked as the top hub gene. In *G. hirsutum*, the expression of *GhNPLA1A* was associated with 361 genes in the WGCNA module (Figure 2f), but *GhNPLA1D* was independent of the module (Figure 2f). It encoded an enzyme that catalyses the hydrolysis of acyl groups from phospholipids to produce free fatty acids (FFAs) and lysophospholipids (LPLs); therefore, it may play important roles during cell elongation in higher plants (Lee et al., 2003). The expression profiles of this gene pair *GhNPLA1A* and *GhNPLA1D* were found to be biased to the A subgenome in *G. hirsutum*: *GhNPLA1A* was highly expressed during the cotton fibre elongation period, while *GhNPLA1D* was almost silenced (Figure 3a, b; Figure S7a and Table S8). However, such biased expression was not observed between *GbNPLA1A* and *GbNPLA1D* in *G. barbadense*

(Figure S7a). Rather, the expression of *GbNPLA1A/D* in elongating cotton fibres reached higher levels and persisted longer than that of *GhNPLA1A/D* (Figure 3c).

Alignment of the coding sequences from *G. hirsutum* and *G. barbadense* revealed a 2-bp deletion in *GhNPLA1D*, but not *GhNPLA1A* and *GbNPLA1A/D* (Figure 3d; Table S9). This deletion led to an early termination of translation and interrupted the lysophospholipase domain (Figure 3e; Figure S8). Ectopic expression of *GhNPLA1A* containing the intact lysophospholipase domain in *Arabidopsis*, driven by the 35S promoter, resulted in seedlings with longer primary roots than the control group (Figure S9). However, ectopic expression of the *GhNPLA1A-N<sup>1-121</sup>* and *GhNPLA1A-C<sup>122-339</sup>*, which contained truncated lysophospholipase domain, resulted in seedlings with similar root lengths to wild type. The above results indicate that this domain is important for fulfilling the function of *GhNPLA1A*. The lower levels of *GhNPLA1D* mRNA may be attributed to non-sense-mediated decay (NMD) (Brognia and Wen, 2009), since the encoded protein may be dysfunctional due to the broken lysophospholipase domain.

Next, the fragment of *GhNPLA1A* and *GhNPLA1D* was cloned using primers designed by SNP between them to investigate the

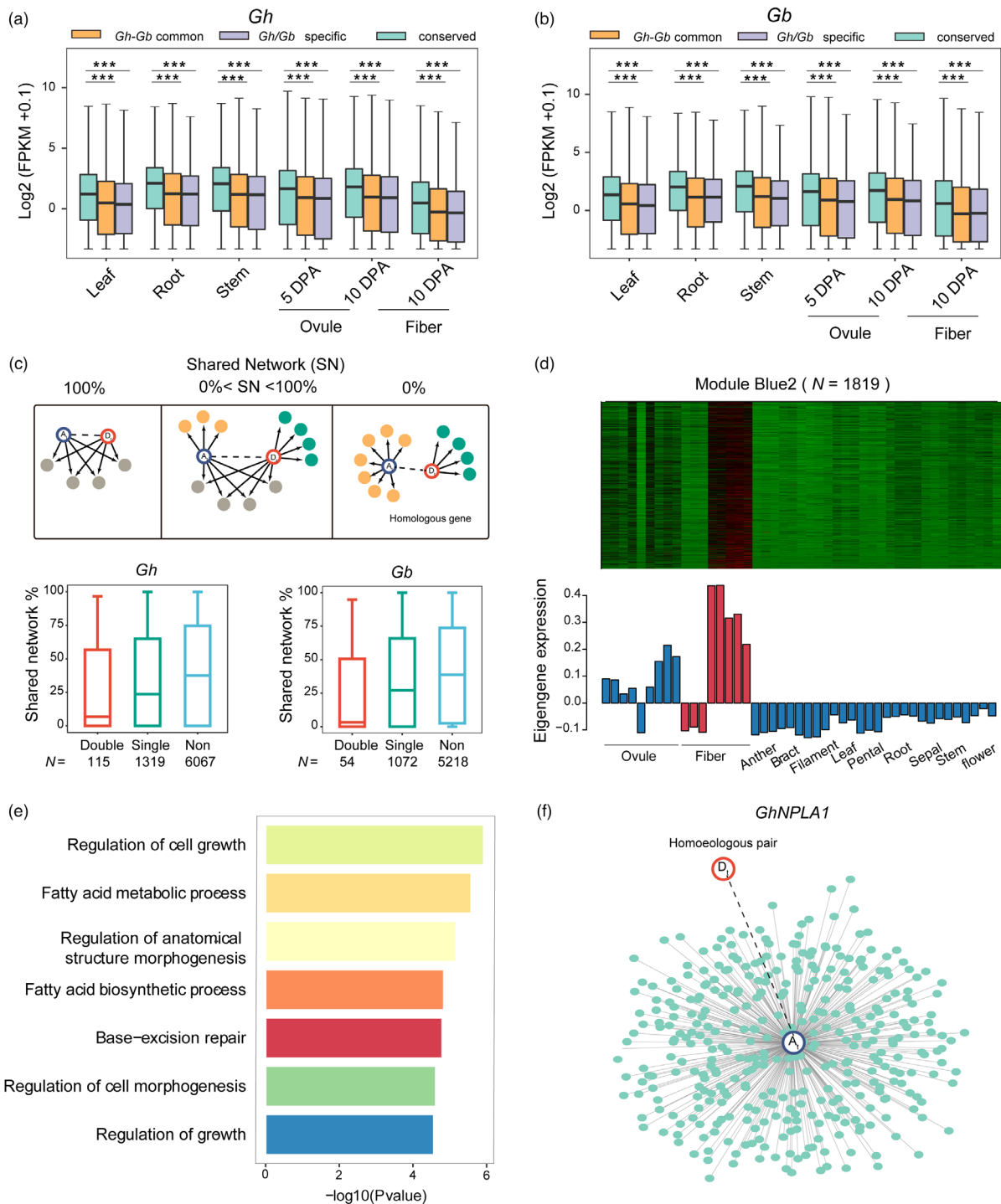


**Figure 2** Alteration of the co-expression networks associated with disrupted genes. (a, b) Comparison of expression levels between disrupted and conserved genes in *G. hirsutum* and *G. barbadense*. Leaf, root, stem, 5-DPA (days post anthesis) ovule, 10-DPA ovule and 10-DPA fibre were selected as representative tissues. Centre line, median; box limits, upper and lower quartiles; whiskers, 1.5× the interquartile range; and dots, outliers (\*\* $p < 0.001$ , \*\*  $p < 0.01$  and \*  $p < 0.05$ , two-tailed t test). (c) Network rewiring between homoeologous genes. Homoeologous genes may have common and unique connections (arrows). Pairs were grouped into whole-share (left), part-share (middle) and zero-share (right) classifications based on the proportion of common connections. Dashed lines indicate homoeologous gene pairs. Shared network proportions between A and D orthologous genes in *G. hirsutum* and *G. barbadense*. The y-axis represents shared connections between homoeologs, and the x-axis, gene type (double, double-disrupted genes; single, single-disrupted genes; and non, conserved genes). Centre line, median; box limits, upper and lower quartiles; whiskers, 1.5× the interquartile range; and dots, outliers. (d) Expression patterns of genes in the fibre-associated module. In the heatmap, red indicates up-regulated genes, black indicates neutral genes, and green indicates down-regulated genes. Bar plots show eigengene values (i.e. the first principal component) calculated from the singular value composition. (e) Gene Ontology enrichment analysis results for genes in the fibre-associated module. (f) Global co-expression network of a homoeologous gene pair (GhNPLA1) in the fibre-associated module. Each dot represents a connected gene.



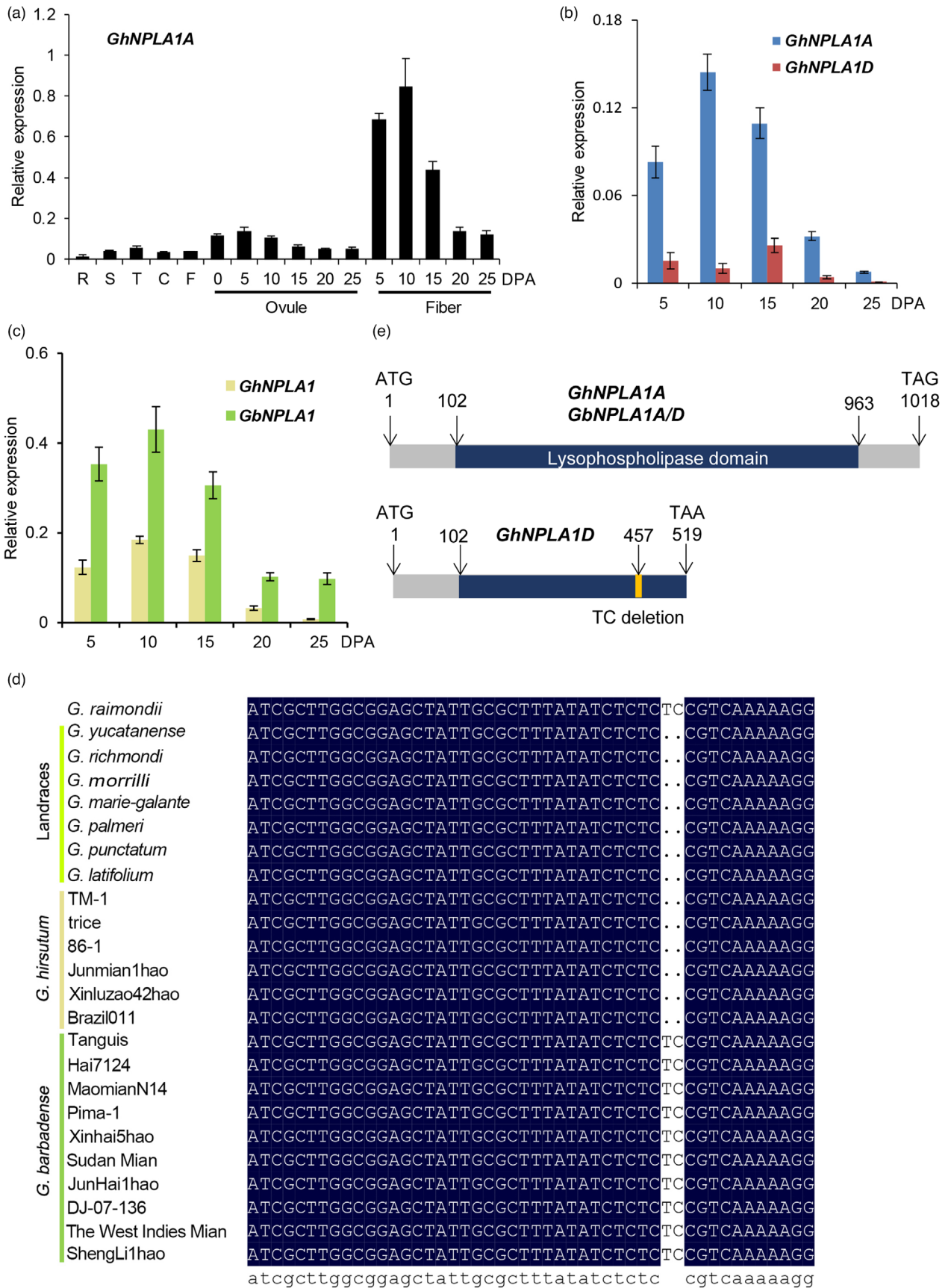


**Figure 3** Expression and structure analysis of the phospholipase A gene in *G. hirsutum* and *G. barbadense*. (a) qRT-PCR analysis of *GhNPLA1A* expression in tissues and organs of *G. hirsutum* acc. TM-1. RNA was isolated from roots (R), stems (S), leaves (L) and cotyledons (C) of two-week-old plants, flowers (F), 0–25 DPA ovules and 5–25 DPA fibres. The *EF-1 $\alpha$*  gene was amplified as a control. Values are means  $\pm$  s.d. ( $n = 3$  biological replicates). (b) qRT-PCR analysis of *GhNPLA1A* and *GhNPLA1D* in *G. hirsutum* acc. TM-1. SNP primers designed to distinguish the homeologs were used for qRT-PCR. (c) qRT-PCR analysis of *GhNPLA1A/D* and *GbNPLA1A/D* expression during fibre development in *G. hirsutum* acc. TM-1 and *G. barbadense* cv. Hai7124. ( $n = 3$  biological replicates). (d) Nucleotide sequence comparison in selected varieties representing *G. raimondii*, *G. hirsutum* and *G. barbadense*. (e) Schematic model of structural variation introduced by the 2-bp deletion. Structures were predicted by Conserved Domain Search in NCBI and showed that GhNPLA1A contained the lysophospholipase domain.

occurrence of this 2-bp deletion variation in *Gossypium* species. Using PCR and Sanger sequencing, the 2-bp deletion was detected in D subgenome of all 70 *G. hirsutum* accessions, which represented 34 landraces and 36 cultivars (Figure 3d and Table S9). Meanwhile, of the 57 *G. barbadense* accessions examined, only two cultivated species contained the deletion; these instances may be due to introgression from *G. hirsutum* during breeding. In order to validate this hypothesis, this 2-bp deletion was examined using cotton populations of 243 diploid accessions (Du *et al.*, 2018) and 3248 tetraploid accession data (He *et al.*, 2021), which were from two public cotton database, GRAND (<http://grand.cricaas.com.cn/>) (Zhang *et al.*, 2022) and CottonGVD (<https://db.cngb.org/cottonGVD/>) (Peng *et al.*, 2021). The 2-bp deletion was only detected in *G. hirsutum* (AD<sub>1</sub>) population, but not in *G. arboreum* population. Thirty accessions of *G. hirsutum* (Han *et al.*, 2022) and *G. barbadense* (Yu *et al.*, 2021) were randomly selected to align their deep resequenced reads to the TM-1 reference genome. Interestingly, the 2-bp deletion was found in all the tested *G. hirsutum* accessions, but not in *G. barbadense* accessions (Table S9).

These findings indicate that the variation identified in *GhNPLA1D* occurred after *Gossypium* speciation. Given its potential roles in cell elongation, variation in *GhNPLA1D* may partially contribute to the difference in fibre length between allotetraploid cottons *G. hirsutum* and *G. barbadense*.

### Retrieving the phospholipase A gene could promote cotton fibre elongation

To compensate for the lost function of the disrupted *GhNPLA1D* gene in fibre cell elongation, we introduced *GhNPLA1A* antisense and overexpression constructs into cotton *via* *Agrobacterium*-mediated transformation (Figure S10a). PCR-based genotyping and kanamycin resistance assays were conducted on the T0-T3 generations until homozygous lines were obtained (Figure S10b and S10c). Three overexpression lines (S4, S6 and S10) and three down-regulation lines (AS3, AS9 and AS10) were selected for further analysis based on expression analysis (Figure 4a). We found that altering the expression of *GhNPLA1A* did not influence cotton growth and development (Figure S10b). However, in comparison with wild-type (WT) and empty vector transgenic control (*pBI121*) plants, the three overexpression lines exhibited longer fibre length at maturity, while the three down-regulation lines had shorter fibre lengths (Figure 4b, c). Measurement of fibre length in S10 and AS10 plants aged 5 to 20 days post-anthesis (DPA) confirmed the significant variation in fibre length compared with WT plants (Figure 4d, e). Thus, elongation rates in S10 and AS10 plants differed from those occurring in WT at the 5–10 DPA and 10–15 DPA periods, during which there was high expression of *GhNPLA1A*. This indicates that *GhNPLA1A* is important in regulating cotton fibre cell elongation.

### *GhNPLA1A* encodes an active phospholipase A

Since GhNPLA1A contained a lysophospholipase domain, we conducted an *in vitro* lysophospholipase activity assay to confirm its functionality. First, we tagged the protein at the N-terminus with maltose-binding protein (MBP) and expressed it in *Escherichia coli* for purification (Figure 5a), then performed the activity assay. The expressed protein released the free C16:0 from the 16:0-lysophosphatidylcholine (LPC) substrate reaction buffer sufficiently (Figure 5b), confirming that GhNPLA1A functions as a lysophospholipase. When 16:0–18:2 phosphatidylcholine (PC) was used as a substrate, production of free 16:0 and 18:2 fatty acids was also observed (Figure 5c), suggesting that GhNPLA1A acts at the sn-1 and sn-2 positions during PC hydrolysis. We also examined the activity of GhNPLA1A against other classes of phospholipids, including phosphatidylinositol (PI), phosphatidylethanolamine (PE), phosphatidic acid (PA) and phosphatidylglycerol (PG). GhNPLA1A hydrolysed all the phospholipids tested, and demonstrated the highest activity when PC was used as the substrate (Figure 5d). These results revealed that GhNPLA1A exhibits typical phospholipase A activity *in vitro*.

### Overexpression of *GhNPLA1A* increased lipid content of cotton fibre

To determine the function of *GhNPLA1A* in lipid metabolism, lipid profiles of 10-DPA fibres from WT, the *GhNPLA1A*-overexpressing line S10 and the *GhNPLA1A*-down-regulated line AS10 were examined *via* mass spectrometry. Free fatty acids (FFAs) and lysophospholipids (LPLs) were taken as potential products of GhNPLA1A activity. In 10-DPA fibres, total FFA levels were 21% higher in S10 and 18% lower in AS10 than in the WT (Figure S11a). The most abundant FFAs were palmitic acid (C16:0) and linolenic acid (C18:3), which constituted 60% of the total FFAs. Contents of all FFA species exhibited a tendency to decrease in AS10 and increase in S10 compared with the WT (Figure S11b). The total LPL level was 15% higher than WT in S10 (Figure S11c, d), but lower in AS10. In cotton fibres, the main species of LPLs were C18:3-LPLs. However, unlike the other species, contents of C18:3-LPLs in AS10 and S10 were not different from that in the WT (Figure S11f-h).

Total phospholipid levels were higher in 10-DPA fibres from AS10, but lower in AS10 plants overall. In addition, PC, PI, PA and PG levels of *GhNPLA1A*-altered plants were significantly different from those of WT plants (Figure 6a-e, Figure S12, and Table S10). In 10-DPA WT fibres, the main phospholipid species were 34:3 and 36:6, both of which contained linolenic acid. There was a general trend towards the content of 34:3 and 36:6 phospholipids being lower in AS10 but higher in S10 compared with WT (Figure 6f-k). In addition, the levels of other phospholipids containing linolenic acid, such as 36:3, 36:4 and 36:5, were also changed. However, total PE content in *GhNPLA1A*-altered

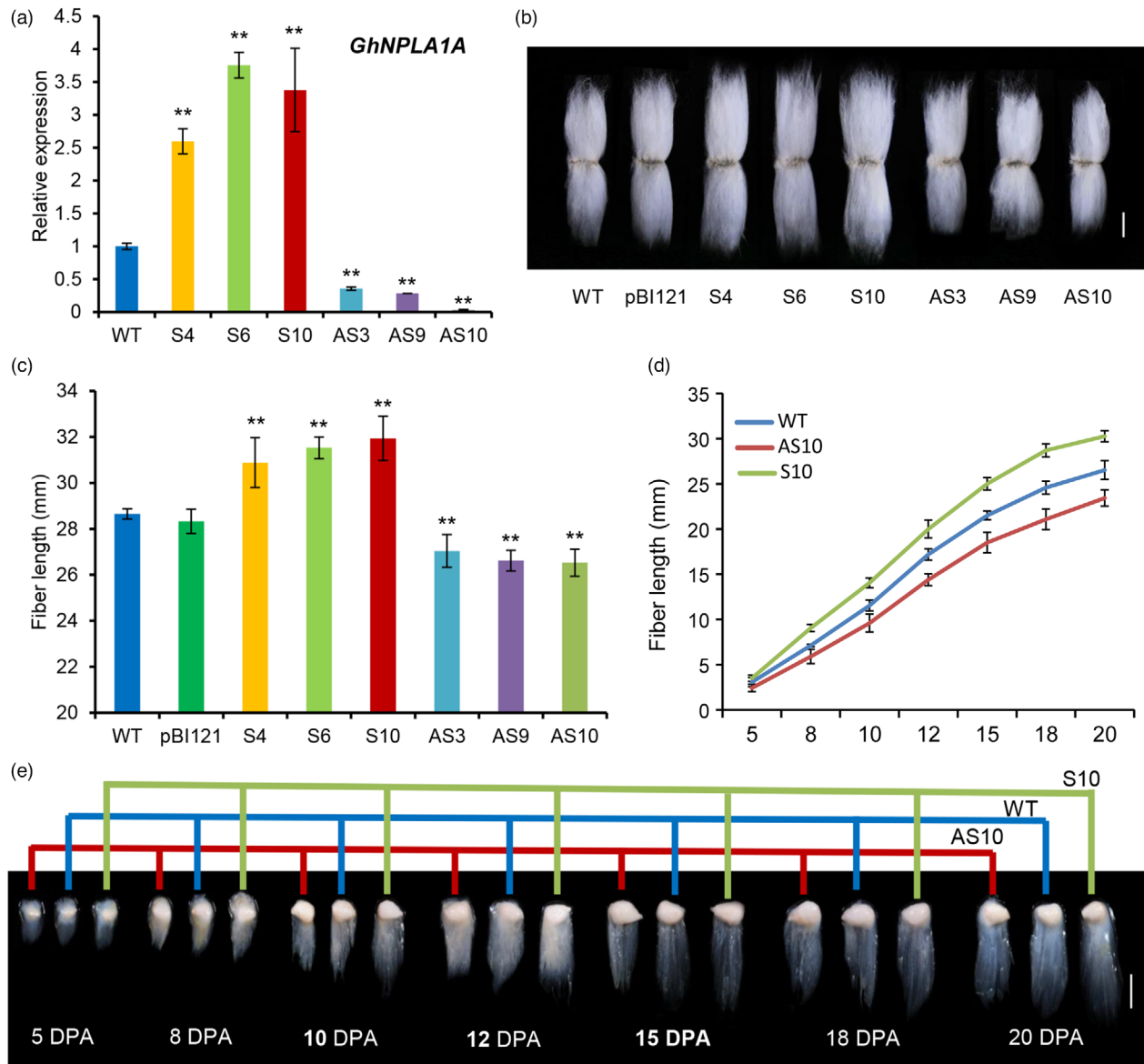


**Figure 4** Ectopic expression of *GhNPLA1* in wild-type upland cotton promotes fibre elongation. (a) Relative expression of *GhNPLA1* in the transgenic cotton. S4, S6 and S10 denote *GhNPLA1* overexpression lines. AS3, AS9 and AS10 are *GhNPLA1*-antisense lines. (b) Photographs showing the mature seed fibre length of the transgenic lines used in panel (a). WT and pBI121 were the transgenic receptor W0 and empty vector transgenic control. (c) Quantitative comparison of fibre lengths in the transgenic cotton lines. Values are means  $\pm$  s.d. ( $n = 3$  biological replicates), \*\* $p < 0.01$ , two-tailed Student's  $t$  test. (d) Fibre elongation of *GhNPLA1A* transgenic lines relative to WT. Values are means  $\pm$  s.d. ( $n = 3$  biological replicates). (e) Phenotypes of fibre-bearing seeds in WT and *GhNPLA1A* transgenic plants. Stages are indicated at the tops of the graphs. Scale bar = 10 mm.

plants was similar to that in WT plants, despite the 34:3 and 36:6 PE contents being higher in S10 than in WT (Figure 6c, h).

#### *GhNPLA1A*-altered fibres respond differently to $\alpha$ -linolenic acid (ALA), 34:3 PI and their inhibitors

ALA ( $\alpha$ -linolenic acid) and 34:3 PI were previously reported to promote fibre elongation, with their inhibitors carboxolone (CBX) and 5-hydroxytryptamine (5-HT) having the opposite role (Liu et al., 2015). In transgenic *GhNPLA1A* cotton fibres, linolenic acid and 34:3 PI contents differed from corresponding values in the WT. Accordingly, we examined the phenotypic variation of cotton fibre elongation in transgenic *GhNPLA1A* plants relating to the effects of ALA, 34:3 PI and their inhibitors using *in vitro* ovule cultures. When 1-DPA ovules were transferred to cultures

containing 5  $\mu$ M ALA and 1  $\mu$ M 34:3 PI, fibre elongation was promoted in all genotypes. However, S10 fibres were more sensitive and AS10 fibres were less sensitive than WT fibres (Figure 7); specifically, fibre elongation was promoted by ~34% and ~40% in S10 plants and ~24% and ~30% in WT plants, but only by ~18% and ~22% in AS10 plants. Treatments with inhibitors, 0.5  $\mu$ M CBX and 0.5  $\mu$ M 5-HT, decreased fibre length to a greater degree. As expected, S10 fibres were less sensitive and AS10 fibres were more sensitive to CBX and 5-HT compared with WT fibres (Figure 7). These results indicated that *GhNPLA1A* promotes *in vivo* fibre elongation, at least in part, by affecting the content of linolenic acid and 34:3 PI. This in turn suggests that *GhNPLA1A* regulate fibre elongation *via* its potential substrate and product content.

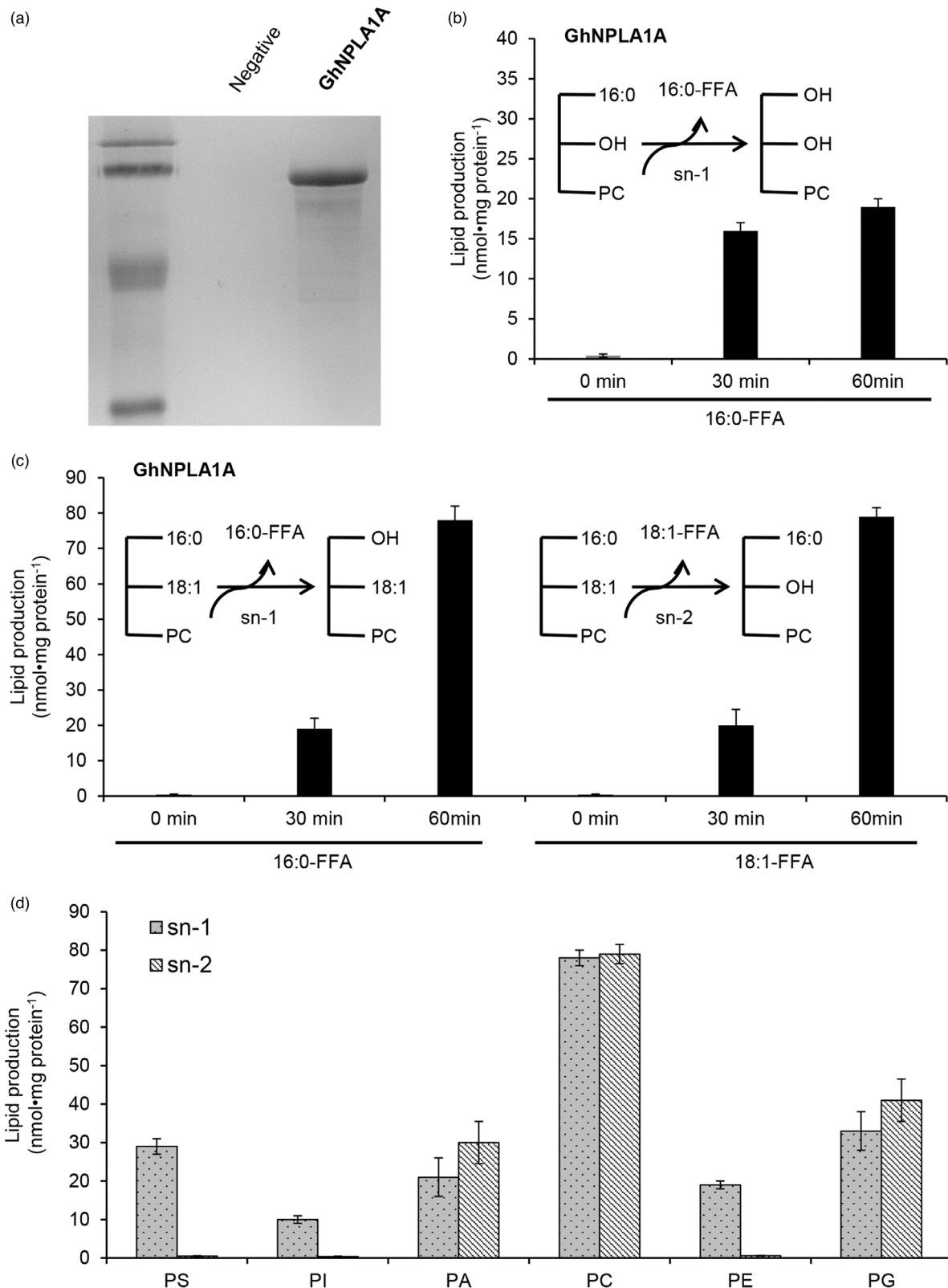


**Figure 5** Purified GhNPLA1A hydrolyses phospholipids *in vitro* at the sn-1 and sn-2 positions. (a) SDS-PAGE loaded with affinity-purified MBP-tag vector and GhNPLA1A from *Escherichia coli*. (b) FFA released by GhNPLA1A when 16:0-LPC vesicles were used as substrate. Values are means  $\pm$  s.d. ( $n = 3$  separate samples). (c) FFA released by GhNPLA1A when 16:0–18:1 PC vesicles were used as substrate. Values are means  $\pm$  s.d. ( $n = 3$  separate samples). (d) Acyl hydrolysis activity of GhNPLA1A towards various classes of phospholipids. Sn-1 and sn-2 were the term representing the fatty acid bond position of triacylglycerin in phospholipids. Vesicles made from individual lipid species were incubated with GhNPLA1A at 28 °C for 60 min. After the reaction, lipids were extracted and quantified by GC/MS. Values are means  $\pm$  s.d. ( $n = 3$  separate samples).



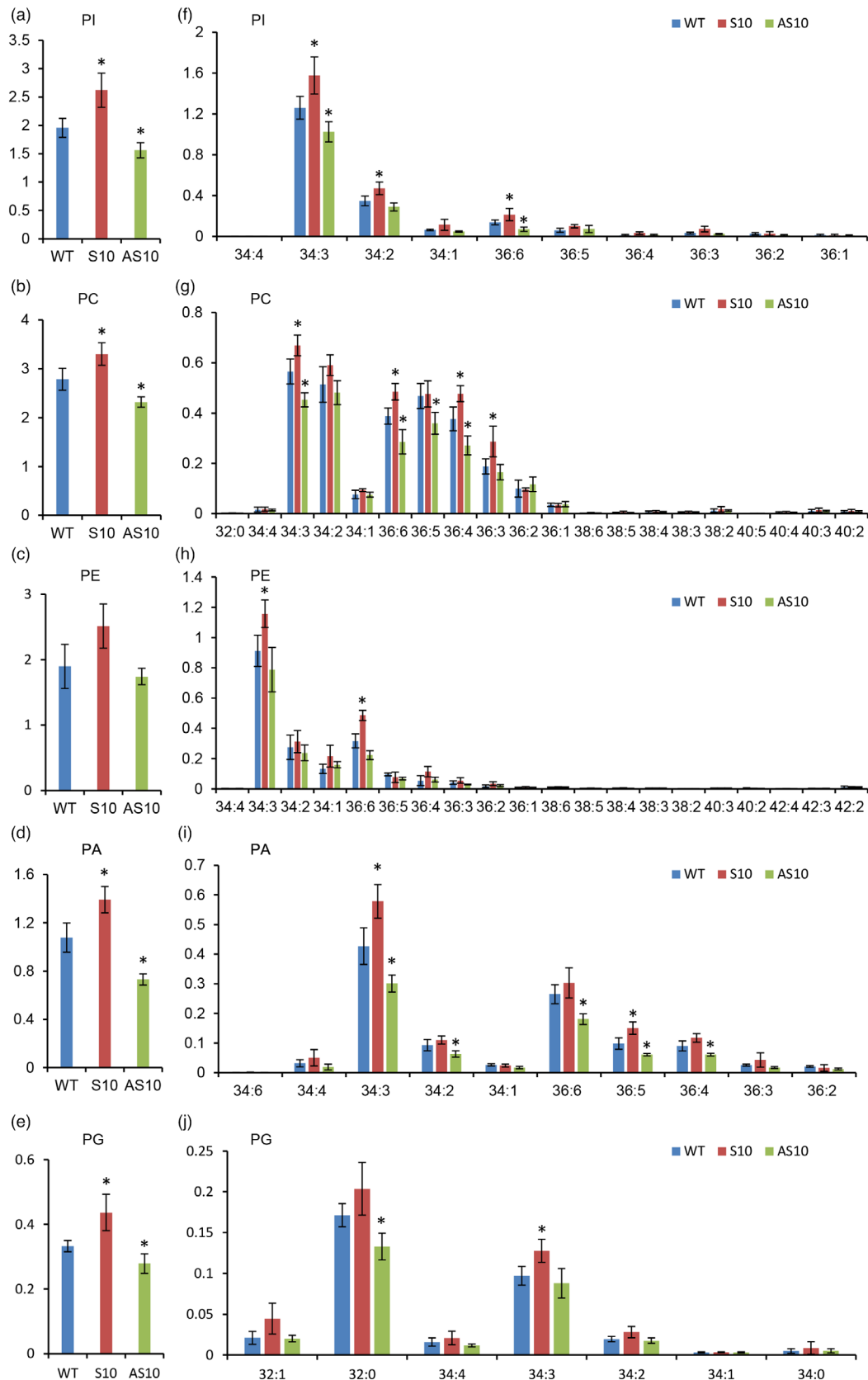
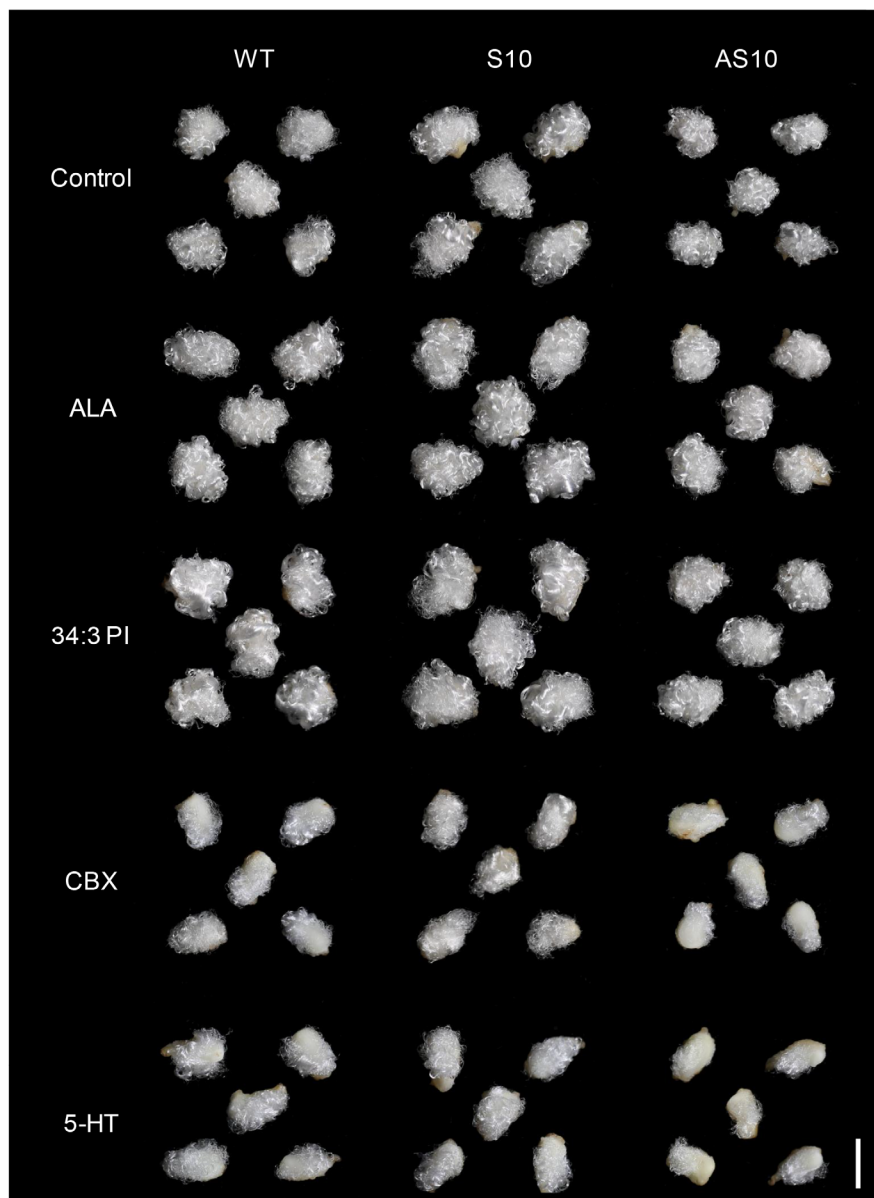
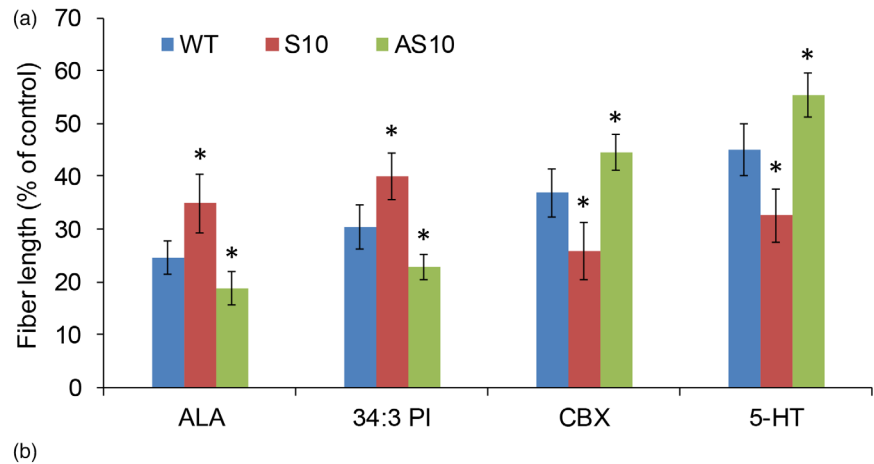


**Figure 6** Effects of altered *GhNPLA1A* expression level on the phospholipid content of cotton fibres. (a–e) Phospholipid content of WT, S10 and AS10 lines. (f–j) Molecular species of phospholipids in WT, S10 and AS10 plants. Phospholipids include PC, PE, PI, PA and PG. Lipids from 10-DPA fibres were quantified by ESI-MS/MS. Values are means  $\pm$  s.d. ( $n = 4$ ). Asterisk indicates a significant difference at  $P < 0.05$  compared with the WT based on Student's *t* test.

**Figure 7** Fibre lengths in S10 and AS10 lines have different sensitivities to ALA, 34:3 PI and their inhibitors. (a) Responses of S10 and AS10 lines to ALA, 34:3 PI, CBX and 5-HT compared with the WT. At least 20 ovules were measured in each case. Error bars indicate the standard deviation of three biological replicates. Asterisks indicate significant difference at  $P < 0.05$  compared with the WT based on Student's *t*-test. (b) Phenotypes of WT, S10 and AS10 ovules cultured for 12 days in BT medium containing 5  $\mu$ M ALA, 1  $\mu$ M 34:3 PI, 0.5  $\mu$ M CBX or 0.5  $\mu$ M 5-HT. Scale bar = 5 mm.



## Discussion

### Gene disruption is parallel to species formation and evolution

Allotetraploids carry pairs of homologues for most genes, which create opportunities by enhancing phenotypic variation (Comai, 2005). Following the ancient polyploidy event in cotton, much genetic redundancy was created, with disrupted genes possibly experiencing different fates. In the present, many disrupted genes with broad-sense inheritance exhibit fast evolution rates, low expression levels and alterable regulation networks. Unlike pseudogenes, we found that most disrupted genes continue to produce RNA; this is probably due to the relative short time passed, evolutionarily speaking, since the formation of tetraploid cotton. Hence, these genes are still undergoing processes of loss-of-function alteration, which relate to methylation and the oxidation–reduction process in cotton polyploidization and *Gh-Gb* speciation history. In WGCNA of homoeologous gene pairs, regulation networks with disrupted genes showed significantly lower correlation coefficients. Genes in the WGCNA modules for fibre development were enriched in the Gene Ontology term metabolic process and regulation of cell growth, indicating a functional bias in gene loss. This indicates that gene disruption could potentially generate different expression patterns and eventually lead to neofunctionalization and subfunctionalization on transcriptional and network levels. We propose that loss of a gene might be accompanied by the alteration or loss of a regulation network that affects traits during evolution. While a ‘polyploidy diversity bottleneck’ arose during cotton allopolyploid formation and speciation because the time interval involved was not sufficient for the accumulation of mutations (Feldman and Levy, 2012), the identified gene disruption events could introduce the genetic diversity of the co-expression network after allopolyploidization, which reflects the dynamic structural and functional plasticity of allopolyploid crops.

### Retrieval of the disrupted gene encoding phospholipase A can restore its functional contribution to fibre enhancement

Loss-of-function events are widely induced and observed in experiments using biotechnological approaches, but it is difficult to extrapolate the functions of genes that have been lost. Here, we discuss three different strategies for studying the functions of disrupted genes. The first is to find, describe and map numerous natural mutants that conditioned yield, quality and resistance traits. Then, functional genes with structural variations can be further fine-mapped and studied. For instance, Ligon lintless-3 mutants have altered lint fibre production, with a mutation in the gene *GhMML4\_D12* causing early termination, resulting in fibreless seeds (Wu *et al.*, 2018). The second strategy is to study how loss of functional genes during polyploidization or domestication could be compensated for using interspecies introgression lines. For example, in rice, small seed size resulting from the loss of the *GL4* gene was compensated using a set of introgression lines between African wild rice and cultivated rice (Wu *et al.*, 2017). Likewise, a maize *UPA2* allele lost during domestication could be compensated by introgression from wild maize to achieve high-density maize yields (Tian *et al.*, 2019). A rapid introgression platform has been used to transfer valuable genomic variations to elite wheat plants, such as presence–absence variations for enhanced resistance (Zhou *et al.*, 2021).

Finally, the new-type *Brassica napus* has been resynthesized to broaden the genetic diversity of *B. napus*, the better to evaluate the impacts of exotic introgression (Hu *et al.*, 2021). The third strategy is to determine how specific gene disruptions could be compensated for using genetic engineering. In this study, we studied a single-lost gene, *GhNPLA1D*, with silenced expression and a lost regulation network, in which the 2-bp deletion causing early termination was exclusively found in the D subgenome of *G. hirsutum*.

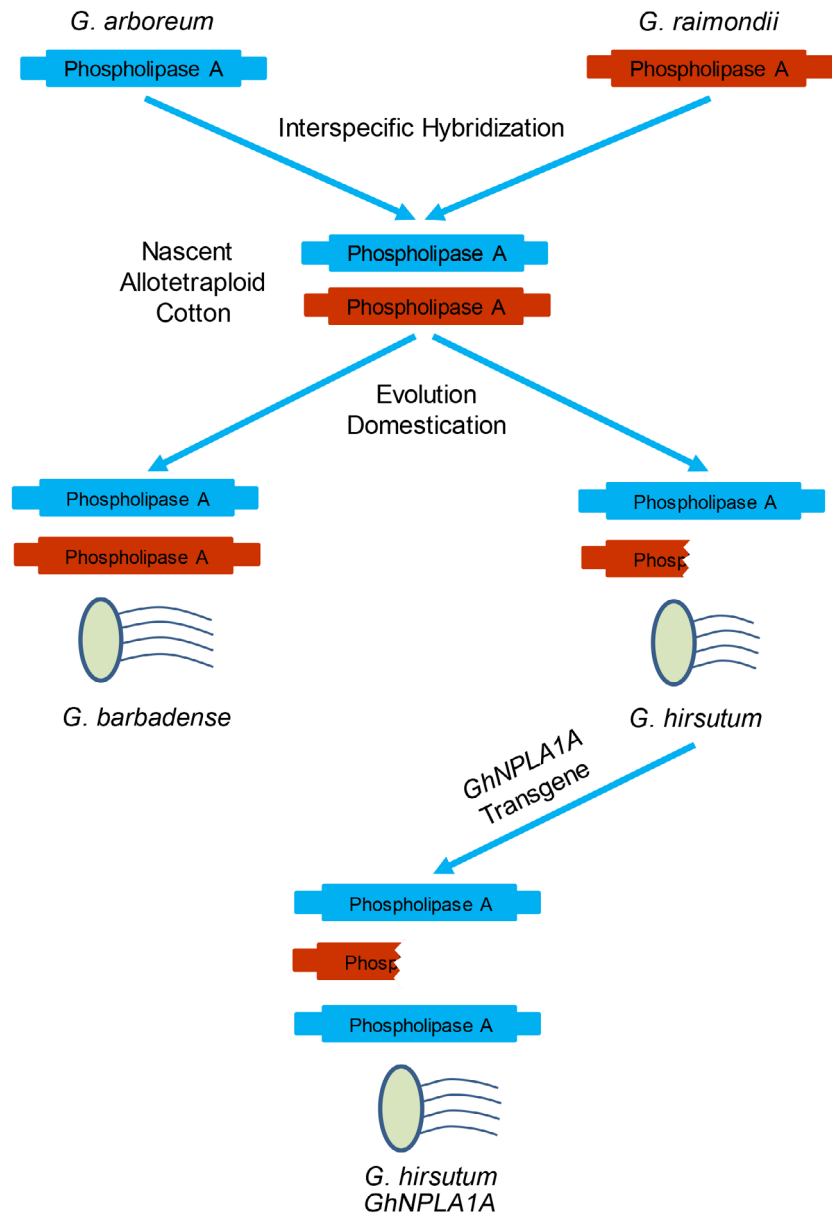
After sequencing 62 *G. barbadense* and 76 *G. hirsutum* accessions, the 2-bp deletion identified here was not observed in the vast majority of *G. barbadense* sequences, despite *G. hirsutum* and *G. barbadense* having both diverged from the nascent allotetraploid cotton that originated in one interspecific hybridization event between diploid species *G. herbaceum* or *G. arboreum* and *G. raimondii* (Du *et al.*, 2018; Huang *et al.*, 2020; Wendel *et al.*, 1995; Wendel *et al.*, 2010; Zhang *et al.*, 2015). However, the 2-bp deletion was also not found in the two diploid progenitor species, A genome *G. arboreum* and D genome *G. raimondii*, demonstrating that the divergence happened after formation of allopolyploid cotton. Overexpression experiments in cotton and *Arabidopsis* demonstrated that *GhNPLA1A* could increase fibre cell length and primary root length, respectively. Meanwhile, reducing the level of *GhNPLA1A* mRNA caused shortened fibres in cotton, indicating that after polyploidization, *G. barbadense* preferred to retain more copies of genes that contribute to fibre elongation than did *G. hirsutum*. The difference in phospholipase A gene could be involved with the molecular basis for the fibre length divergence in these two allopolyploid cottons (Figure 8).

### *GhNPLA1A* accelerates phospholipid biosynthesis *in vivo* by hydrolysing phospholipids containing the linolenic acid moiety to promote fibre elongation

*GrNPLA1*, the ancestor of *GhNPLA1A* in *G. raimondii*, is phylogenetically clustered with *AtMAGL1*, *AtMAGL3/AtLysoPL2*, *AtMAGL14* and *AtMAGL16* (Figure S7b), which belong to the monoacylglycerolase gene family. However, the proteins encoded by these genes have no monoacylglycerolase activity in *Arabidopsis* (Kim *et al.*, 2016). Instead, *AtMAGL1* and *AtLysoPL2* exhibit lysophospholipase activity (Gao *et al.*, 2010; Kim *et al.*, 2016). Here, enzyme activity assays revealed that the protein encoded by *GhNPLA1A* has phospholipase A activity *in vitro*. When fibre expression of *GhNPLA1A* was altered using transgenic methods, the content of phospholipids, and of their hydrolysis products LPLs and FFAs, changed correspondingly showing that *GhNPLA1A* encodes a novel phospholipase A in cotton *in vivo*. The content of total FFAs and LPLs was positively related to the expression of *GhNPLA1A*. However, unlike other LPLs, LPLs containing linolenic acid in *GhNPLA1A-S* and *GhNPLA1A-AS* lines remained similar to values in the WT. Exploiting this interested result, combined with the changes in the content of linolenic acid, we presumed that *GhNPLA1A* prefers to hydrolyse phospholipids containing linolenic acid *in vivo*; otherwise, LPLs containing linolenic acid should also change if *GhNPLA1A* hydrolyses phospholipids containing another FA moiety (Figure S13).

Correspondingly, phospholipid analysis found *GhNPLA1A*-altered cotton fibres also showed altered content of phospholipids containing linolenic acid and confirmed our conjecture. However, contrary to expectation, these levels tended to be lower

**Figure 8** Evolution model of phospholipase A gene and its consequences for fibre elongation in cotton. The genomes of the two diploid ancestor species, *G. arboreum* and *G. raimondii*, each harbours normal phospholipase A gene. After formation of a nascent allotetraploid cotton from the interspecific hybridization of *G. arboreum* and *G. raimondii*, *G. hirsutum* and *G. barbadense* diverged and evolved independently. In this process, *G. barbadense* retained two copies of *GhNPLA1* and developed extra-staple fibres, while *G. hirsutum* lost one copy of *GhNPLA1D* and produced short fibres. The restored *GhNPLA1A* copy number in transgenic *G. hirsutum* achieved the longer fibre phenotype.



in *GhNPLA1A*-AS fibres and higher in *GhNPLA1A*-S fibres relative to WT fibres. This finding is counterintuitive, considering that *GhNPLA1A* hydrolyses phospholipids *in vitro*. In *Arabidopsis*, *pPLAIII $\delta$*  encodes a protein that showed typical phospholipase A activity, and overexpression of this gene increased total phospholipid content (Chen *et al.*, 2013; Li *et al.*, 2013). Similarly, overexpression of the related *pPLAIII $\beta$*  also increased phospholipid content by accelerating phospholipid biosynthesis (Li *et al.*, 2011). These reported results could explain the paradox that *GhNPLA1A* functions as typical phospholipase A to accelerate phospholipid containing linolenic acid biosynthesis in cotton fibres.

Unlike other plant cell types, the predominant molecular species of PC, PE, PI and PA in cotton fibres were 34:3 (16:0, 18:3) and 36:6 (18:3, 18:3) (Li *et al.*, 2011; Liu *et al.*, 2015; Wanjie *et al.*, 2005), indicating that cotton fibres feature active synthesis and metabolism of phospholipids containing the linolenic acid moiety. Linolenic acid and 34:3 PI, but not other long-chain fatty acids and phospholipids, were found to promote

fibre elongation *in vitro* (Liu *et al.*, 2015; Qin *et al.*, 2007). Furthermore, while Li *et al.* (2011) reported that treatment of *Arabidopsis* seedlings with linolenic acid at 50  $\mu$ M or 100  $\mu$ M inhibited primary root growth, a later study in cotton found that linolenic acid at 5  $\mu$ M and 34:3 PI at 1  $\mu$ M could promote fibre elongation. Transgenic and genetic evidences show that *GhNPLA1* plays a positive role in cotton fibre elongation. We also found *GhNPLA1A*-S plants have higher contents of linolenic acid and 34:3 PI relative to WT, while *GhNPLA1A*-AS plants had lower contents. We then tested the effect of linolenic acid, 34:3 PI and their inhibitors on cotton fibres *in vitro* and found that both linolenic acid and 34:3 PI promote cotton fibre elongation, while their inhibitors inhibit cotton fibre elongation. Furthermore, *GhNPLA1A*-S fibres were more sensitive to linolenic acid and 34:3 PI than wild-type fibres, whereas AS fibres were less sensitive. And these relative sensitivities were reversed when treating ovules with the inhibitors. Therefore, the effect of *GhNPLA1A* on fibre length may result, at least in part, from the elevated intracellular levels of linolenic acid and 34:3 PI. All polyploids, including

palaeopolyploids, recent allopolyploids and diloidized autopolyploids, have undergone cytological and genetic diploidization (Feldman and Levy, 2012). Although many genes are disrupted in this process and subsequently continue to be lost through the genomic accumulation of mutations and through domestication, genetic population mapping and function studies have succeeded in partly demonstrating the previous functions of such genes. Our work opens the door to a strategy for identifying disrupted genes and retrieving their lost functions in ways that can provide valuable resources for accelerating trait enhancement in cotton breeding.

## Methods

### Identification of disrupted genes from genome sequences

Disrupted genes were traced between an allotetraploid and its presumed diploid wild ancestor. The selected taxa included *G. hirsutum*, *G. barbadense*, *G. arboreum* and *G. raimondii*. Genome data for each selected taxon were obtained from the COTTONGEN database (<https://www.cottongen.org/>) (Yu *et al.*, 2014) and Cotton Omics Database (<http://cotton.zju.edu.cn/>). To reduce computational complexity, sequences of *G. hirsutum* and *G. barbadense* (Hu *et al.*, 2019) were divided into subgenomes: *GhAt*, *GhDt*, *GbAt* and *GbDt*. Reads were assigned to the diploid ancestor's relatives *G. arboreum* (Du *et al.*, 2018; Huang *et al.*, 2020) and *G. raimondii* (Paterson *et al.*, 2012) using the software BWA (Li and Durbin, 2009). Only uniquely mapping reads were retained. Following alignment, we used the Indel Realigner from the Genome Analysis Toolkit to correct alignment errors near indels and identify SNPs and indels (McKenna *et al.*, 2010). In the obtained variant calling format files, heterozygous sites and those missing in one sample were considered as misalignments and were excluded from further analysis. Deleterious variants were annotated using ANNOVAR (Wang *et al.*, 2010b). Genes were considered disrupted if identified as containing stop-gain, stop-loss, frameshift deletion or frameshift insertion variants. The deleterious variants were also annotated using another software SnpEff (v 3.5) (<http://snpeff.sourceforge.net/>) with default parameters (Cingolani *et al.*, 2012) in order to conform the accuracy of genomic variation annotations.

### Identification of orthologs

We constructed one-to-one homoeolog families in which all members were homoeologous genes in cotton and rape using OrthoFinder (parameters were -M msa -S blast -I 4 -t 5) (Emms and Kelly, 2019). This yielded a set of 20 096 orthologous *Gossypium* gene pairs (*Ga*: *Gr*: *GhA<sub>i</sub>*: *GhD<sub>i</sub>*: *GbA<sub>i</sub>*: *GbD<sub>i</sub>*), the lists of which can be found in Table S2.

### Calculation of Ka, Ks and Ka/Ks

To evaluate the levels of selective constraint on the disrupted genes, we determined the numbers of synonymous sites (Ks) and non-synonymous sites (Ka) between each post-polyploidization gene and its diploid counterparts. Protein alignments were generated using pairwise ClustalW (Larkin *et al.*, 2007). Multiple sequence alignments were transformed using ParaAT (Zhang *et al.*, 2012). Synonymous nucleotide substitutions on synonymous sites were estimated using the Nei–Gojobori approach (Nei and Gojobori, 1986) to implement the Ka/Ks calculator (Wang *et al.*, 2010a).

### Estimating the expression levels of disrupted genes

The cotton RNA-seq data used in this study had been generated by our laboratory previously (Hu *et al.*, 2019; Zhang *et al.*, 2015). Briefly, these data were derived from 45 different tissues spanning the developmental stages of *G. hirsutum* and *G. barbadense*. The accession numbers and samples are given in Table S3. To determine which lost genes were potentially transcribed, we determined the fragments per kilobase of transcripts per million mapped fragments (FPKM) value of each gene. RNA-seq data were preprocessed, and quality control was applied using Fastp to filter out adapters and low-quality sequences (Chen *et al.*, 2018). Clean data were aligned against a reference genome using the software HISAT2 (-dta) (Pertea *et al.*, 2016). The gene expression in each sample was estimated and quantified in FPKM by StringTie (-e -G) (Pertea *et al.*, 2016). An FPKM value greater than 0.5 in all the examined samples was considered to be detectable.

### Degrading the gene co-expression network

The expression levels of disrupted genes and conserved genes were examined in selected representative tissues: cotton leaf, root, stem, sepal, 1-DPA ovule, 3-DPA ovule, 5-DPA ovule, 10-DPA ovule, 10-DPA fibre, 20-DPA fibre and 25-DPA fibre. To study the co-expression patterns among conserved–conserved, disrupted–conserved and disrupted–disrupted homoeologous pairs, we calculated Spearman's correlations of expression levels across different samples using `cor()` and `cor.test()` in R.

Co-expression network analysis has emerged as a very useful approach for functional annotation. It is based on the idea that all genes involved in a particular biological pathway will be connected to each other. Here, gene co-expression networks were constructed using the R package WGCNA (v1.63) (Langfelder and Horvath, 2008). Genes in a one-to-one relationship of *G. hirsutum* and *G. barbadense* were imported for analysis, and further divided into 17 modules and 12 modules, respectively. Genes in the blue2 module of *G. hirsutum* are listed in Table S5. Module–trait associations were estimated using the correlations between the eigengene module and ovule and fibre samples.

### Validation the disrupted gene *GhNPLA1D* using population data

The 2-bp deletion causing early termination of *GhNPLA1D* was validated in 57 *G. barbadense* and 70 *G. hirsutum* accessions using PCR and Sanger sequencing. Primers were designed from the flanking sequences according to the 2-bp deletion positions in the *GhNPLA1D* (Table S9), which presents the real sequences unbiased by any short-read assembly. The amplification profile consisted of an initial denaturation step at 94 °C for 4 min, followed by 35 cycles of 94 °C for 30 s, 58 °C for 30 s and 72 °C for 40 s, with a final extension step at 72 °C for 10 min.

The 2-bp deletion was also detected in two cotton databases, GRAND (<http://grand.cricaas.com.cn/>) (Zhang *et al.*, 2022) and CottonGVD (<https://db.cngb.org/cottonGVD/>) (Peng *et al.*, 2021), including 243 diploid cotton accessions genome data (Du *et al.*, 2018) and 3000 cotton genome data (He *et al.*, 2021). Moreover, from previous published data, 30 *G. hirsutum* (Han *et al.*, 2022) and 30 *G. barbadense* individuals (Yu *et al.*, 2021) (Table S9) were randomly selected and their resequenced data were aligned against to the TM-1 reference genome using BWA (Li and Durbin, 2009). Only uniquely mapping reads were retained. Following alignment, we used



the Indel Realigner from the Genome Analysis Toolkit to correct alignment errors near indels and identify SNPs and indels (McKenna *et al.*, 2010).

### Plant materials, growth conditions and cotton ovule cultures

This study used the cotton cultivars *G. hirsutum* acc. W0. The plants were grown in our Jiangpu breeding field in Nanjing, China. Ovule and fibre stages were identified by tagging each pedicel on the day of flowering, and samples representing the different stages were removed carefully from developing bolls for DNA, RNA and lipid extraction. This study also used *Arabidopsis* cultivar Columbia-0 as transgenic receptor, in which plants were grown in a growth chamber or glasshouse with long-day conditions (22 °C, 16 h of light and ~70% relative humidity). Cotton ovules were cultured according to the method described by Beasley (Beasley, 1971). After surface sterilization using 75% ethanol, cotton ovules collected from bolls at 1 DPA were cultured in liquid BT medium at 30 °C in the presence of 5 µM linolenic acid, 1 µM 34:3 PI, 0.5 µM CBX and 0.5 µM 5-HT (Liu *et al.*, 2015).

### Gene expression analysis and gene cloning

The genome and transcriptome data of *G. hirsutum* acc. TM-1 were obtained from our laboratory as described by Zhang *et al.* (2015) (NCBI database, SRA: PRJNA248163). The genome and transcriptome data of *G. barbadense* cv. Hai7124 were also obtained from our laboratory (Hu *et al.*, 2019). The data were visualized using the MeV software (Saeed *et al.*, 2003). *GhNPLA1A* sequences were amplified from the cDNA of 5-DPA *G. hirsutum* acc. TM-1 fibres using gene-specific primers (Table S11). The SNP primers used to detect the 2-bp deletion were developed from *GhNPA1A* and *GhNPLA1D* sequences using WebSNAPER (<https://pga.mgh.harvard.edu/cgi-bin/snap3/websnaper3.cgi>).

### Enzyme assays

Hydrolase activity was measured by monitoring the release of FFA from 1,2-dimyristoyl-sn-glycero-3-phosphate (sodium salt) (DMPA), 1-palmitoyl-2-oleoyl-sn-glycero-3-phosphocholine (POPC), 1-palmitoyl-2-oleoyl-sn-glycero-3-phosphoethanolamine (POPE), 1-palmitoyl-2-oleoyl-sn-glycero-3-phospho-(1'-rac-glycerol)(POPG), l- $\alpha$ -phosphatidylinositol (PI) and 1-palmitoyl-2-hydroxy-sn-glycero-3-phosphocholine (LPC) (Aladdin). To conduct the assay, 50 µg of each substrate in chloroform was first evaporated under vacuum for 10 min. Then, 500 µL of reaction buffer (50 mM Tris-HCl, pH 8.0, 1 mM dithiothreitol) was added and vortexed vigorously, and the suspension was further sonicated for 10 min in a water bath sonicator. Afterwards, 100 µL of each substrate mixture was pre-warmed to 28 °C for half an hour. The reaction was initiated by adding 20 µg of purified MBP-tagged GhNPLA1A protein, then incubated at 28 °C for different time intervals, and was stopped by the addition of 300 µL Dole reagent (isopropanol: heptane: 2 M sulphuric acid = 3000: 750: 150). The FFAs released from each substrate were extracted by first adding 300 µL heptane and 300 µL water, then aliquoting 200 µL of the heptane phase and evaporating it. To methylate the isolated FFAs, 300 µL of 0.4 M potassium hydroxide in methanol was added and incubated for 30 min at room temperature. After adding 700 µL of heptane and 300 µL of water, the methylated fatty acids were extracted and measured by GC/MS. For quantitation of both palmitic and oleic acid methyl esters, a known amount of

POPC was directly methylated and extracted by the method described above, then serially diluted.

### Real-time quantitative RT-PCR (qRT-PCR)

qRT-PCR was carried out according to the method described by Zhang *et al.* (2017). The primers used to detect expression of *GhNPLA1A/D* genes in the At and Dt subgenomes were designed using WebSNAPER (<http://pga.mgh.harvard.edu/cgi-bin/snap3/websnaper3.cgi>) based on a single nucleotide polymorphism (SNP) in the *GhNPLA1A/D* exon. The gene used as internal control was *EF-1 $\alpha$* . Three biological replicates were used for each reaction with two technical replicates each. Mean values and standard errors were calculated according to data from three replicates. The primers used for qRT-PCR are listed in Table S11.

### Vector construction and plant transformation

The pBI121 plasmid was used as the backbone for vector construction. Two pairs of primers (*GhNPLA1A*-full-F and *GhNPLA1A*-full-R) were used to amplify the full-length cDNA sequence, and the pairs OE-*GhNPLA1A*-F/R and AS-*GhNPLA1A*-F/R were used to amplify coding sequence for insertion into the pBI121 plasmid to construct *GhNPLA1A* overexpression/suppression vectors, both of which were driven by the constitutive Cauliflower Mosaic Virus 35S promoter (CaMV 35S). The vectors were then transformed into *G. hirsutum* acc. W0 as described previously (Wu *et al.*, 2008). Kanamycin selection coupled with PCR-based genotyping was used to determine the homozygosity of transgenic plants. The primers used for vector construction and PCR-based screening are listed in Table S11.

### Lipid content analysis of cotton fibres

Lipids were extracted and analysed by electrospray ionization–tandem mass spectrometry (ESI-MS/MS), and levels of PA, PC, PE, PG, PI and PS were determined using a method described previously (Liu *et al.*, 2015). LPC, LPE and LPG were determined by a method described previously (Li *et al.*, 2011). FFAs were determined by ESI-MS, using heptadecanoic acid (C17:0) as an internal standard (Sigma-Aldrich), scanning in the negative ion mode over the mass range of m/z 200 to m/z 350.

### Acknowledgements

This study was financially supported in part by grants from the NSFC (32172008, 31822036), Project of Hainan Yazhou Bay Seed Lab (B21HJ0223), a project from Sanya Yazhouwan Technology City (SKJC-2021-02-001), the Leading Innovative and Entrepreneur Team Introduction Program of Zhejiang (2019R01002), the Fundamental Research Funds for the Central Universities (226-2022-00153) and Research Startup Funding from Hainan Institute of Zhejiang University (0202-6602-A12201).

### Competing interests

The authors declare no competing financial interests.

### Author contributions

L.F. and T. Zhang conceptualized the research program. L.F., Z.Z., T. Zhao, H.M., F.W., Z.H., N.Z., Z.S. and Y.H. performed bioinformatics analyses. L.F., T. Zhao, X.H., X.G., S.Z. and S.L. analysed all the data. L.F., Z.Z., T. Zhao and T. Zhang wrote the

manuscript. All authors discussed results and commented on the manuscript.

## Data availability

All sequenced genomic data and transcriptomic data can be downloaded from the Cotton Omics Database (<http://cotton.zju.edu.cn/>).

## References

- Adams, K.L. and Wendel, J.F. (2005) Polyploidy and genome evolution in plants. *Curr. Opin. Plant Biol.* **8**, 135–141.
- Arsovski, A.A., Pradinuk, J., Guo, X.Q., Wang, S. and Adams, K.L. (2015) Evolution of cis-regulatory elements and regulatory networks in duplicated genes of *Arabidopsis*. *Plant Physiol.* **169**, 2982–2991.
- Beasley, C.A. (1971) In-vitro culture of fertilized cotton ovules. *Bioscience*, **21**, 906–907.
- Brogna, S. and Wen, J.K. (2009) Nonsense-mediated mRNA decay (NMD) mechanisms. *Nat. Struct. Mol. Biol.* **16**, 107–113.
- Chen, G., Greer, M.S. and Weselake, R.J. (2013) Plant phospholipase a: advances in molecular biology, biochemistry, and cellular function. *Biomol. Concepts*, **4**, 527–532.
- Chen, S., Zhou, Y., Chen, Y. and Gu, J. (2018) Fastp: an ultra-fast all-in-one FASTQ preprocessor. *Bioinformatics*, **34**, i884–i890.
- Chen, Z.J. and Guan, X. (2011) Auxin boost for cotton. *Nat. Biotechnol.* **29**, 407–409.
- Cingolani, P., Platts, A., Wang le, L., Coon, M., Nguyen, T., Wang, L., Land, S.J. *et al.* (2012) A program for annotating and predicting the effects of single nucleotide polymorphisms, SnpEff. *Fly*, **6**, 80–92.
- Comai, L. (2005) The advantages and disadvantages of being polyploid. *Nat. Rev. Genet.* **6**, 836–846.
- Conover, J.L. and Wendel, J.F. (2022) Deleterious mutations accumulate faster in allopolyploid than diploid cotton (*Gossypium*) and unequally between subgenomes. *Mol. Biol. Evol.* **39**, msac024.
- Du, X., Huang, G., He, S., Yang, Z., Sun, G., Ma, X., Li, N. *et al.* (2018) Resequencing of 243 diploid cotton accessions based on an updated a genome identifies the genetic basis of key agronomic traits. *Nat. Genet.* **50**, 796–802.
- Emms, D.M. and Kelly, S. (2019) OrthoFinder: phylogenetic orthology inference for comparative genomics. *Genome Biol.* **20**, 238.
- Fang, L., Zhao, T., Hu, Y., Si, Z., Zhu, X., Han, Z., Liu, G. *et al.* (2021) Divergent improvement of two cultivated allotetraploid cotton species. *Plant Biotechnol. J.* **19**, 1325–1336.
- Feldman, M. and Levy, A.A. (2012) Genome evolution due to allopolyploidization in wheat. *Genetics*, **192**, 763–774.
- Gao, W., Li, H.Y., Xiao, S. and Chye, M.L. (2010) Acyl-CoA-binding protein 2 binds lysophospholipase 2 and lysoPC to promote tolerance to cadmium-induced oxidative stress in transgenic *Arabidopsis*. *Plant J.* **62**, 989–1003.
- Gou, J.Y., Wang, L.J., Chen, S.P., Hu, W.L. and Chen, X.Y. (2007) Gene expression and metabolite profiles of cotton fiber during cell elongation and secondary cell wall synthesis. *Cell Res.* **17**, 422–434.
- Graves, D.A. and Stewart, J.M. (1988) Analysis of the protein constituency of developing cotton fibers. *J. Exp. Bot.* **39**, 59–69.
- Guan, X., Lee, J.J., Pang, M., Shi, X., Stelly, D.M. and Chen, Z.J. (2011) Activation of *Arabidopsis* seed hair development by cotton fiber-related genes. *PLoS One*, **6**, e21301.
- Han, Z., Chen, H., Cao, Y., He, L., Si, Z., Hu, Y., Lin, H. *et al.* (2022) Genomic insights into genetic improvement of upland cotton in the world's largest growing region. *Ind. Crop Prod.* **183**, 114929.
- He, S., Sun, G., Geng, X., Gong, W., Dai, P., Jia, Y., Shi, W. *et al.* (2021) The genomic basis of geographic differentiation and fiber improvement in cultivated cotton. *Nat. Genet.* **53**, 916–924.
- Hu, D.D., Zhao, Y.S., Shen, J.X., He, X.X., Zhang, Y.K., Jiang, Y., Snowdon, R. *et al.* (2021) Genome-wide prediction for hybrids between parents with distinguished difference on exotic introgressions in *Brassica napus*. *Crop J.* **9**, 1169–1178.
- Hu, Y., Chen, J., Fang, L., Zhang, Z., Ma, W., Niu, Y., Ju, L. *et al.* (2019) *Gossypium barbadense* and *Gossypium hirsutum* genomes provide insights into the origin and evolution of allotetraploid cotton. *Nat. Genet.* **51**, 739–748.
- Huang, G., Wu, Z., Percy, R.G., Bai, M., Li, Y., Frelichowski, J.E., Hu, J. *et al.* (2020) Genome sequence of *Gossypium herbaceum* and genome updates of *Gossypium arboreum* and *Gossypium hirsutum* provide insights into cotton A-genome evolution. *Nat. Genet.* **52**, 516–524.
- Kim, H.J. and Triplett, B.A. (2001) Cotton fiber growth in planta and in vitro. Models for plant cell elongation and cell wall biogenesis. *Plant Physiol.* **127**, 1361–1366.
- Kim, R.J., Kim, H.J., Shim, D. and Suh, M.C. (2016) Molecular and biochemical characterizations of the monoacylglycerol lipase gene family of *Arabidopsis thaliana*. *Plant J.* **85**, 758–771.
- Langfelder, P. and Horvath, S. (2008) WGCNA: an R package for weighted correlation network analysis. *BMC Bioinformatics*, **9**, 559.
- Larkin, M.A., Blackshields, G., Brown, N.P., Chenna, R., McGettigan, P.A., McWilliam, H., Valentin, F. *et al.* (2007) Clustal W and Clustal X version 2.0. *Bioinformatics*, **23**, 2947–2948.
- Lee, H.Y., Bahn, S.C., Kang, Y.M., Lee, K.H., Kim, H.J., Noh, E.K., Palta, J.P. *et al.* (2003) Secretory low molecular weight phospholipase A2 plays important roles in cell elongation and shoot gravitropism in *Arabidopsis*. *Plant Cell*, **15**, 1990–2002.
- Li, H. and Durbin, R. (2009) Fast and accurate short read alignment with burrows-wheeler transform. *Bioinformatics*, **25**, 1754–1760.
- Li, M., Bahn, S.C., Fan, C., Li, J., Phan, T., Ortiz, M., Roth, M.R. *et al.* (2013) Patatin-related phospholipase pPLAIII $\Delta$  increases seed oil content with long-chain fatty acids in *Arabidopsis*. *Plant Physiol.* **162**, 39–51.
- Li, M., Bahn, S.C., Guo, L., Musgrave, W., Berg, H., Welti, R. and Wang, X. (2011) Patatin-related phospholipase pPLAIII $\beta$ -induced changes in lipid metabolism alter cellulose content and cell elongation in *Arabidopsis*. *Plant Cell*, **23**, 1107–1123.
- Liu, G.J., Xiao, G.H., Liu, N.J., Liu, D., Chen, P.S., Qin, Y.M. and Zhu, Y.X. (2015) Targeted lipidomics studies reveal that linolenic acid promotes cotton fiber elongation by activating phosphatidylinositol and phosphatidylinositol monophosphate biosynthesis. *Mol. Plant*, **8**, 911–921.
- Lynch, M. and Conery, J.S. (2000) The evolutionary fate and consequences of duplicate genes. *Science*, **290**, 1151–1155.
- McKenna, A., Hanna, M., Banks, E., Sivachenko, A., Cibulskis, K., Kernytzky, A., Garimella, K. *et al.* (2010) The genome analysis toolkit: a MapReduce framework for analyzing next-generation DNA sequencing data. *Genome Res.* **20**, 1297–1303.
- Nei, M. and Gojobori, T. (1986) Simple methods for estimating the numbers of synonymous and nonsynonymous nucleotide substitutions. *Mol. Biol. Evol.* **3**, 418–426.
- Paterson, A.H., Wendel, J.F., Gundlach, H., Guo, H., Jenkins, J., Jin, D., Llewellyn, D. *et al.* (2012) Repeated polyploidization of *Gossypium* genomes and the evolution of spinnable cotton fibres. *Nature*, **492**, 423–427.
- Peng, Z., Li, H., Sun, G., Dai, P., Geng, X., Wang, X., Zhang, X. *et al.* (2021) CottonGVD: a comprehensive genomic variation database for cultivated cottons. *Front. Plant Sci.* **12**, 803736.
- Pertea, M., Kim, D., Pertea, G.M., Leek, J.T. and Salzberg, S.L. (2016) Transcript-level expression analysis of RNA-seq experiments with HISAT, StringTie and ballgown. *Nat. Protoc.* **11**, 1650–1667.
- Qin, Y.M., Hu, C.Y., Pang, Y., Kastaniotis, A.J., Hiltunen, J.K. and Zhu, Y.X. (2007) Saturated very-long-chain fatty acids promote cotton fiber and *Arabidopsis* cell elongation by activating ethylene biosynthesis. *Plant Cell*, **19**, 3692–3704.
- Saeed, A., Sharov, V., White, J., Li, J., Liang, W., Bhagabati, N. *et al.* (2003) TM4: a free, open-source system for microarray data management and analysis. *Biotechniques*, **34**, 374–378.
- Snel, B., Bork, P. and Huynen, M.A. (2002) Genomes in flux: the evolution of archaeal and proteobacterial gene content. *Genome Res.* **12**, 17–25.

- Tian, J., Wang, C., Xia, J., Wu, L., Xu, G., Wu, W., Li, D. *et al.* (2019) Teosinte ligule allele narrows plant architecture and enhances high-density maize yields. *Science*, **365**, 658–664.
- Wang, D., Zhang, Y., Zhang, Z., Zhu, J. and Yu, J. (2010a) KaKs\_Calculator 2.0: a toolkit incorporating gamma-series methods and sliding window strategies. *Genom. Proteom. Bioinf.* **8**, 77–80.
- Wang, K., Li, M. and Hakonarson, H. (2010b) ANNOVAR: functional annotation of genetic variants from high-throughput sequencing data. *Nucleic Acids Res.* **38**, e164.
- Wanjie, S.W., Welti, R., Moreau, R.A. and Chapman, K.D. (2005) Identification and quantification of glycerolipids in cotton fibers: reconciliation with metabolic pathway predictions from DNA databases. *Lipids*, **40**, 773–785.
- Wendel, J.F., Brubaker, C.L. and Seelanan, T. (2010) The origin and evolution of *Gossypium*. In *Physiology of Cotton* (Stewart, J., Oosterhuis, D., Heitholt, J. and Mauney, J., eds), pp. 1–18. Dordrecht: Springer.
- Wendel, J.F., Schnabel, A. and Seelanan, T. (1995) An unusual ribosomal DNA sequence from *Gossypium gossypoides* reveals ancient, cryptic, intergenomic introgression. *Mol. Phylogenet. Evol.* **4**, 298–313.
- Wu, H., Tian, Y., Wan, Q., Fang, L., Guan, X., Chen, J., Hu, Y. *et al.* (2018) Genetics and evolution of MIXTA genes regulating cotton lint fiber development. *New Phytol.* **217**, 883–895.
- Wu, S.J., Wang, H.H., Li, F.F., Chen, T.Z., Zhang, J., Jiang, Y.J., Ding, Y.Z. *et al.* (2008) Enhanced agrobacterium-mediated transformation of *embryogenic calli* of upland cotton via efficient selection and timely subculture of somatic embryos. *Plant Mol. Biol. Rep.* **26**, 174–185.
- Wu, W., Liu, X., Wang, M., Meyer, R.S., Luo, X., Ndjondjop, M.N., Tan, L. *et al.* (2017) A single-nucleotide polymorphism causes smaller grain size and loss of seed shattering during African rice domestication. *Nat. Plants*, **3**, 17064.
- Yang, L., Takuno, S., Waters, E.R. and Gaut, B.S. (2011) Lowly expressed genes in *Arabidopsis thaliana* bear the signature of possible pseudogenization by promoter degradation. *Mol. Biol. Evol.* **28**, 1193–1203.
- Yu, J., Jung, S., Cheng, C.H., Ficklin, S.P., Lee, T., Zheng, P., Jones, D. *et al.* (2014) CottonGen: a genomics, genetics and breeding database for cotton research. *Nucleic Acids Research*, **42**, 1229–1236.
- Yu, J., Hui, Y., Chen, J., Yu, H., Gao, X., Zhang, Z., Li, Q. *et al.* (2021) Whole-genome resequencing of 240 *Gossypium barbadense* accessions reveals genetic variation and genes associated with fiber strength and lint percentage. *Theor. Appl. Genet.* **134**, 3249–3261.
- Zhang, T., Hu, Y., Jiang, W., Fang, L., Guan, X., Chen, J., Zhang, J. *et al.* (2015) Sequencing of allotetraploid cotton (*Gossypium hirsutum* L. acc. TM-1) provides a resource for fiber improvement. *Nat. Biotechnol.* **33**, 531–537.
- Zhang, Z., Ruan, Y.L., Zhou, N., Wang, F., Guan, X., Fang, L., Shang, X. *et al.* (2017) Suppressing a Putative Sterol Carrier Gene Reduces Plasmodesmal Permeability and Activates Sucrose Transporter Genes during Cotton Fiber Elongation. *Plant Cell*, **29**, 2027–2046.
- Zhang, Z., Xiao, J., Wu, J., Zhang, H., Liu, G., Wang, X. and Dai, L. (2012) ParaAT: a parallel tool for constructing multiple protein-coding DNA alignments. *Biochem. Biophys. Res. Commun.* **419**, 779–781.
- Zhang, Z., Chai, M., Yang, Z., Yang, Z. and Fan, L. (2022) GRAND: an integrated genome, transcriptome resources, and gene network database for *Gossypium*. *Front. Plant Sci.* **13**, 773107.
- Zhou, Y., Bai, S., Li, H., Sun, G., Zhang, D., Ma, F., Zhao, X. *et al.* (2021) Introgressing the *Aegilops tauschii* genome into wheat as a basis for cereal improvement. *Nat. Plants*, **7**, 774–786.

## Supporting information

Additional supporting information may be found online in the Supporting Information section at the end of the article.

**Figure S1.** Distribution of deleterious variation in different species.

**Figure S2.** Distribution of disrupted genes across the cotton genome.

**Figure S3.** Genomic features of disrupted genes related to polyploidization and speciation.

**Figure S4.** Distribution of Pearson correlation coefficients between A and D homoeologous genes.

**Figure S5.** Matrix showing Module-trait relationship of different modules in different *G. hirsutum* tissues.

**Figure S6.** Matrix showing Module-trait relationship of different modules in different *G. barbadense* tissues.

**Figure S7.** The expression and sequence characteristics of *GhNPLA1A* in cotton.

**Figure S8.** Amino acid sequence alignment of *GhNPLA1* and *GbNPLA1* in TM-1 and Hai7124.

**Figure S9.** Overexpression of *GhNPLA1A* but not *GhNPLA1A-N* and *GhNPLA1A-C* caused the longer primary root length in seedling development of *Arabidopsis*.

**Figure S10.** *GhNPLA1A* constructs used for genetic transformation.

**Figure S11.** The effect of alterations in *GhNPLA1A* on FFA and LPL content in cotton fibres.

**Figure S12.** Principal component analysis of each phospholipid content in WT, S10 and AS10 plants.

**Figure S13.** *GhNPLA1A* may prefer to hydrolyse the linolenic acid from phospholipids containing the linolenic acid moiety *in vivo* based on the content of the LPLs and FFAs in *GhNPLA1A*-altered cotton fibre.

**Table S1.** Identification of variants associated with gene disruption.

**Table S2.** List of one-to-one homoeologous genes in *Gossypium*.

**Table S3.** Statistics of RNA-seq libraries in this study.

**Table S4.** List of double-disrupted and single-disrupted genes.

**Table S5.** Gene list of fibre associated module blue2.

**Table S6.** GO analysis of the module blue2.

**Table S7.** Single-lost genes within extremely changed co-expression network.

**Table S8.** FPKM values of *GhNPLA1* and *GbNPLA1* in TM-1 and Xinhai21.

**Table S9.** Distribution of 2 bp deletion in cotton genome.

**Table S10.** Pearson coefficient correlation analysis of four duplicated experiments of each phospholipid content.

**Table S11.** Oligonucleotides used for gene cloning, qRT-PCR and vector construction in this study.